Kondo Universal Scaling for a Quantum Dot Coupled to Superconducting Leads

C. Buizert,[1] A. Oiwa,[1] K. Shibata,[2] K. Hirakawa,[2] and S. Tarucha[1,3,*]

[1]*Department of Applied Physics, University of Tokyo, 7-3-1 Hongo, Bunkyo-ku, 113-8656, Japan*
[2]*IIS, University of Tokyo, 4-6-1 Komaba, Meguro-ku, Tokyo 153-8505, Japan*
[3]*Quantum Spin Information Project, ICORP, Japan Science and Technology Agency, Atsugi-shi, Kanagawa 243-0198, Japan*

(Received 10 June 2007; published 28 September 2007)

We study competition between the Kondo effect and superconductivity in a single self-assembled InAs quantum dot contacted with Al lateral electrodes. Because of Kondo enhancement of Andreev reflections, the zero-bias anomaly develops side peaks, separated by the superconducting gap energy Δ. For ten valleys of different Kondo temperature T_K we tune the gap Δ with an external magnetic field. We find that the zero-bias conductance in each case collapses onto a single curve with Δ/k_BT_K as the only relevant energy scale, providing experimental evidence for universal scaling in this system.

DOI: 10.1103/PhysRevLett.99.136806 PACS numbers: 73.21.La, 72.15.Qm, 74.45.+c

The concept of universality evolved from the study of phase transitions in the field of statistical mechanics, where it was found that critical phenomena can be grouped in classes. All systems within the same universality class show identical behavior near the critical point for a certain set of relevant observables, despite the differences in microscopic details of the systems at hand [1]. Although formally not a phase transition, the Kondo effect has been shown to exhibit universality as well [2]. The Kondo effect arises from the antiferromagnetic interaction of localized magnetic impurities with conduction electrons. Below a characteristic temperature, the Kondo temperature T_K, a strongly correlated many-body state is formed that screens the impurity and greatly increases its scattering cross section [3]. The last ten years have seen a renewed interest in this phenomenon with the possibility to use the unpaired electron spin on a quantum dot (QD) as the impurity, a setup that offers unprecedented control over experimental parameters [4,5].

Kondo universality manifests itself as the governance of the Kondo energy scale k_BT_K over all low-energy physics of the system. Other scales, such as the charging energy U_C or lead coupling Γ, can be an order of magnitude larger, yet to describe the response to external parameters we require only T_K and G_0, the zero temperature conductance. Under influence of a finite temperature, bias voltage or magnetic field ($X = k_BT$, eV_{SD} or $g\mu_BB$) the normalized conductance $G(X)/G_0$ is reduced monotonically from unity following a curve that scales only with X/k_BT_K [6]. Once appropriately scaled the behavior of any microscopic realization of the Kondo model can be collapsed onto this curve. The prime example of Kondo universality is its temperature dependence, where the empirical function

$$G(T)/G_0 = [1/(1 + (T/T_K^*)^2)]^s \qquad (1)$$

is widely used to fit experimental data. Here $T_K^* = T_K/\sqrt{2^{1/s} - 1}$, to conform with the definition of the Kondo temperature $G(T_K) = G_0/2$, and $s = 0.22$ for spin-1/2 systems [7]. Once expressed in the dimensionless parameters $G(T)/G_0$ and T/T_K the behavior of, e.g., semiconductor based dots [7], carbon nanotubes [8,9] and single-molecule transistors [10] could be mapped onto curve 1, showing the dominance of T_K over the system's microscopic details.

Both superconductivity and the Kondo effect are many-body interactions with a strict inherent spin ordering. In a regular *s*-wave superconductor the electrons condense in singlet Cooper pairs, whereas the Kondo ground state consists of a dynamic many-body singlet formed between the localized dot electron and the itinerant lead electrons. Their competition is characterized by the relative strength Δ/k_BT_K; for $\Delta/k_BT_K \ll 1$ the Kondo effect can survive in the presence of superconducting (SC) leads, in the opposite limit $\Delta/k_BT_K \gg 1$ Kondo is suppressed restoring Coulomb blockade (CB). The possibility of Andreev scattering at the dot-SC interface results in an even richer physics. Through multiple Andreev reflections (MAR) a Cooper pair of charge $2e$ can be transported across the dot [11]. In the Kondo regime a resonant channel opens up at the Fermi level, making the dot more transparent for the MAR processes. This allows the conductance to exceed the unitary limit of $2e^2/h$, provided that T_K exceeds Δ [12]. This surprising prediction was confirmed experimentally by Buitelaar *et al.* [9] for a carbon nanotube with Al electrodes. They observed a crossover between enhancement and suppression of the Kondo conductance at $k_BT_K \approx \Delta$, explained with a resistively-shunted junction model [13]. We work in a different regime where MAR is strongly damped by repulsive Coulomb interactions, though we will see that first order AR is enhanced by the Kondo effect. In contrast to Ref. [9] the zero-bias conductance is suppressed over the entire range of Kondo temperatures by the gap Δ at the Fermi level.

We shall study transport through a single self-assembled InAs quantum dots contacted laterally via the nanogap method [14] to Al SC electrodes. The dots are formed by molecular-beam epitaxy deposition of ~4 ML InAs on a

GaAs substrate; at this coverage many individual dots have coalesced into larger InAs islands with a diameter of ~80 nm. The source and drain contacts, separated by a 25 nm gap, are defined by e-beam lithography. e-beam deposition of Ti (5 nm) and Al (100 nm) is preceded by a 5 s buffered hydrofluoric acid etching step to deoxidize the surface. Roughly 5% of the gaps are bridged by a dot, yielding a working device [Fig. 1(c)]. Each Al electrode is doubly contacted, allowing 4-terminal measurements. A degenerately doped layer 300 nm below the surface acts as an electrostatic backgate. Using a 4-terminal Al test strip deposited simultaneously we can characterize the Al leads to have a critical temperature $T_C = 0.9$ K and critical field $B_C = 95$ mT in perpendicular orientation. More details of the fabrication process will be given elsewhere [15].

The measurements presented were done on a device with a RT junction resistance of 100 kΩ. First we apply a 100 mT field to suppress superconductivity in the electrodes. Figure 1(a) shows the charge stability diagram (Coulomb diamond) of the device, where we control the number of electrons on the dot with the voltage V_G applied to the back gate. Figure 1(b) shows the linear response at zero bias. We find a dot charging energy $U_C \sim 2.5$ meV and an electronic level spacing $\delta E \sim 2.5$ meV. Counting the Coulomb oscillations we obtain an electron occupancy

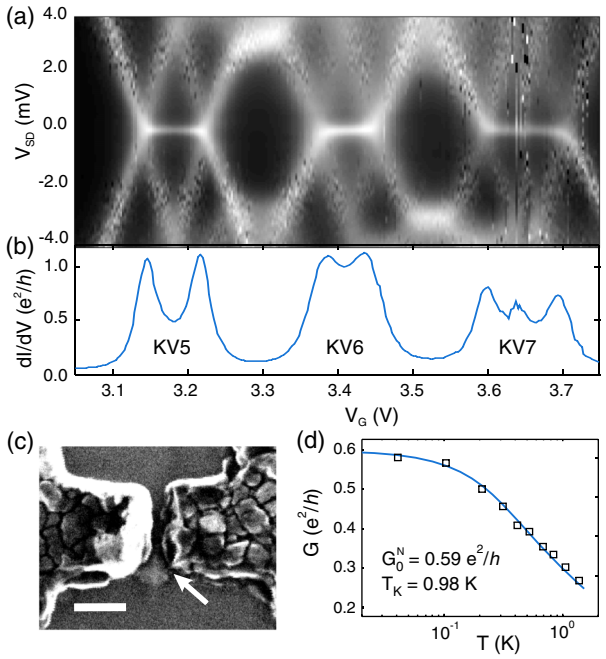

FIG. 1 (color online). (a) Differential conductance dI/dV_{SD} as a function of V_G and V_{SD}, with the leads driven normal by a field $B = 100$ mT. $T = 35$ mK. (b) dI/dV_{SD} at $V_{SD} = 0$ mV in units of e^2/h. We show KV5 to KV7 with a T_K of 1.04, 1.65, and 1.18 K, respectively. (c) Scanning electron micrograph of a similar device as used in these studies, with 100 nm scale bar. An InAs dot bridges the source and drain electrodes. (d) Temperature dependence of the conductance at KV5, with a best fit to scaling curve 1.

of $N = 12$ for the leftmost valley at $V_G = 3.0$ V. Around $V_G = 3.64$ V we reproducibly suffer from an electrostatic switch in the environment, which we attribute to the charging of a nearby InAs dot.

The stability diagram clearly exhibits the even-odd parity associated with the spin-1/2 Kondo effect, showing an enhanced conductance ridge around zero bias for odd occupancy. For the various Kondo valleys the value of T_K is different each time, as the electronic orbitals couple differently to the reservoirs. In addition to this variation, thermal cycling to room temperature also alters the dot parameters, including T_K. Divided over three cool downs of the device, we were able to study 10 different values of T_K, ranging from 0.7 to 2 K. We shall refer to them as Kondo valley (KV) 1–10. For KV5 the zero-bias conductance is shown as a function of temperature in Fig. 1(d); the line shows a best fit to the empirical curve 1. The fitting gives $T_K = 0.98$ K, which is close to the value of 1.04 K found from half the width of the Kondo resonance out of equilibrium. From now on we shall use the latter method to determine T_K. The maximum normal state conductance G_0^N was always smaller than $2e^2/h$, indicating an asymmetric lead coupling.

Sweeping back to zero magnetic field we bring the electrodes in the SC state. Figure 2(a) shows the zero field Coulomb diamond. For even occupancy two parallel lines at source-drain (SD) bias $|V_{SD}| = 2\Delta/e$ mark the onset of direct quasiparticle tunneling. Their separation of 4Δ allows us to determine $\Delta = 0.14$ meV, in good agreement with the critical temperature of the leads via the BCS relation $\Delta(T = 0) = 1.76 k_B T_C$ [16]. An accurate scan of the gap structure at even electron number is shown in Fig. 2(b), the peaks at $|V_{SD}| = 2\Delta/e$ reflect the singularity in the density of states (DOS) of the leads. The MAR found in other QD devices connected to SC-leads [17,18] is here absent due to strong on-site Coulomb interaction between the carriers ($U_C \sim 17\Delta$) [19]. Only the first order Andreev reflection at $|V_{SD}| = \Delta/e$ is faintly visible as a shoulder to the 2Δ feature.

We now turn to the behavior in the Kondo regime. The transition from the N to SC state with the magnetic field is shown in Fig. 2(c). With the leads in the N-state the field splits the Kondo resonance; we observe a peak in the differential conductance when V_{SD} equals the Zeeman energy [4]. A linear fit gives a g factor $|g| = 6.6 \pm 0.3$. Below B_C we surprisingly observe three resonances in the differential conductance. The two nonequilibrium ones occur at $|V_{SD}| = \Delta/e$, reflecting the SC DOS of the leads. Their position follows the field dependence of Δ, being maximum at zero field. This conspicuous positioning corresponds to the first order Andreev reflection (AR), the physical process where an incoming electron scatters at the N-SC interface, injecting a Cooper pair in the SC region and a back reflected hole in the N region [16]. Through an interaction with the Kondo effect the AR is enhanced

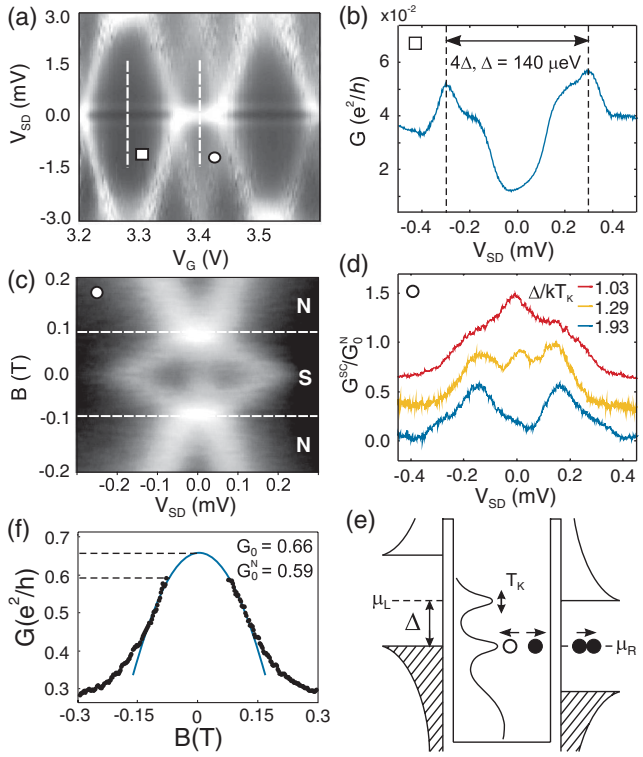

FIG. 2 (color online). (a) dI/dV_{SD} as a function of V_G and V_{SD}, with the leads in the SC state ($B = 0$ T). (b) Scan of the gap structure in the CB regime, as indicated by the square in upper figure. Conductance is suppressed for $V_{SD} < 2\Delta$. (c) Color-scale plot of dI/dV_{SD}, showing the field dependence of the Kondo resonance (KV2, $T_K = 1.23$ K). Horizontal lines denote the SC-N transition in the leads. (d) The Kondo resonance out of equilibrium for three different Kondo valleys (KV 10,2,4 from upper to lower) with the leads in the SC state. The curves are normalized by their N-state conductance G_0^N. Offset for clarity. (e) Schematic depiction of the Kondo enhanced Andreev Reflection, with a split Kondo resonance in the dot DOS. (f) Zero-bias Kondo conductance (KV2) as a function of magnetic field, with N-state leads.

[13,20]; the mechanism is depicted schematically in Fig. 2(e). In the middle of the valleys charge fluctuations are inhibited and the electrons traverse the dot through cotunneling processes. In the CB regime the lowest available state is $\sim(U_C + \delta E)/2$ away, but, by contrast, in the Kondo regime the many-body resonance gives rise to a finite DOS at the Fermi energy, enhancing the conductance. At finite bias the Kondo DOS splits with a maximum at each lead chemical potential, for $V_{SD} = \Delta/e$ this maximum aligns exactly with the band edge of the opposite reservoir. The electrons that contribute to the AR tunnel at this energy, and in this way the first order AR is strongly enhanced by the Kondo effect.

In Fig. 2(d) we compare the normalized conductance G^{SC}/G_0^N as a function of V_{SD} for 3 different valleys. Surprisingly, the height $G^{SC}|_\Delta$ of the satellites appears to be insensitive to Δ/k_BT_K, and was between 0.65 and $0.9G_0^N$ for all 10 values of T_K studied. A very recent work by Sand-Jespersen [21] reports on similar Kondo enhanced AR in dots of small T_K. Why this process can persist where $\Delta \gg k_BT_K$ is uncertain. We speculate that the exact alignment with the band edge allows an out-of-equilibrium recovery of the Kondo state similar to the case of an applied magnetic field. Note that the direct tunneling onset at $|V_{SD}| = 2\Delta/e$ is not enhanced by Kondo, and its features are dwarfed by the much larger Δ peaks.

In contrast to the Δ satellites the zero-bias conductance is very sensitive to the relative strength Δ/k_BT_K, or the ability of the Kondo effect to break up lead spin-pairing. For $\Delta \simeq k_BT_K$ (upper graph) the zero-bias conductance is close to its N-state value, whereas for higher Δ/k_BT_K the SC gap suppresses the conductance increasingly. Note that the resonance around $V_{SD} = 0$ cannot be interpreted as a supercurrent, as was done by Grove-Rasmussen *et al.* [22]. A low critical current $I_C \sim 100$ pA is to be expected as the Cooper pairs of charge $2e$ cannot tunnel directly due to the high U_C. The lead noise temperature of $\sim$100 mK is roughly 10 times higher than the Josephson energy $E_J = \hbar I_C/2e$, destroying SC phase coherence across the junction. Indeed no dissipationless flow was detected in a current biased 4-terminal measurement.

We analyze the 10 separate Kondo valleys, each with a different T_K. On top of that we use the magnetic field to alter the SC gap, providing us a knob to experimentally tune Δ/k_BT_K. By comparison, using the V_G dependence of T_K as a knob gives a much smaller range of variation. In Fig. 3 we have plotted G^{SC}/G_0^N at different fields as a function of Δ/k_BT_K. When plotted in this fashion all data points collapse onto a single curve, proving that

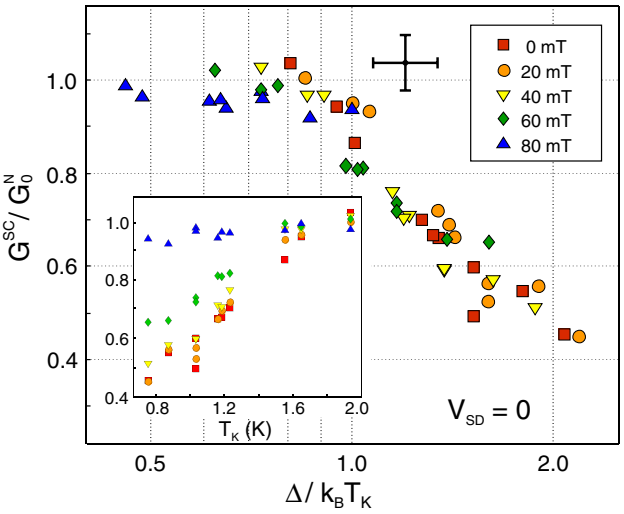

FIG. 3 (color online). Semilog plot of G^{SC}/G_0^N for KV1–10 at various fields. Plotted against Δ/k_BT_K, the data collapse on a single curve. The field dependent value of Δ was 135, 140, 120, 100, and 60 μeV for 0, 20, 40, 60, and 80 mT, respectively. The measurement uncertainty is given by the bars. Inset shows the same data plotted against T_K only.

Δ/k_BT_K is the only relevant scaling parameter for the system. For comparison the inset shows the same data set as a function of just T_K. The scaling curves for other external parameters, such as temperature [23], bias [24], or irradiation [25] ($X = k_BT$, eV_{SD} and $\hbar\omega$), are characterized by a logarithmic conductance falloff in the weak coupling regime ($X \gg k_BT_K$) where a perturbative approach is valid. Although the data range is too limited to unambiguously claim any functional form, the observed falloff seems to agree with the expected logarithmic dependence. Fitting the data with an empirical form such as function 1 gives a poor correspondence. However, the k_BT and Δ scaling curves need not be the same as the underlying mechanism is fundamentally different. Furthermore, we believe the shape of the curve to be slightly distorted by the magnetic field, as discussed later on. In contrast to the results of Buitelaar [9] we always find that the gap Δ suppresses the zero-bias conductance, also in the regime $k_BT_K > \Delta$. The main difference is the strong Coulomb repulsion in our device that damps the MAR, the latter being necessary to raise G^{SC} above G_0^N. Unfortunately, the field behavior is not discussed in Ref. [9], making a direct comparison difficult.

To shed some light on the origin of the observed scaling we want to point out a similarity with the effect of other perturbations. Under equilibrium conditions the spin-flip cotunneling processes that create the Kondo singlet conserve energy. At finite V_{SD} or k_BT there is phase space available to inelastic processes, leading to decoherence of the many-body Kondo state [24,25]. In the case of SC leads, a spin-flip with the leads requires the breaking of a Cooper pair, creating two excitations in the conduction band. This cost of 2Δ requires energy exchange with the environment, leading to a suppressed conductance through decoherence of the Kondo singlet.

Finally, we want to address the non-negligible Zeeman splitting caused by the field that tunes Δ. At 80 mT it equals $E_Z = 30$ μeV, which should be compared to the Kondo energy k_BT_K that ranges from 70 to 170 μeV. The suppression of the conductance by the splitting depends on both $|B|$ and T_K, and, consequently, we can expect the shape of the observed scaling function to be slightly distorted. Furthermore, we used G_0^N at 100 mT, rather than the ''true'' G_0, for normalization. In Fig. 2(f) we have plotted the equilibrium conductance of KV2 as a function of magnetic field, with the SC leads regime omitted. In the absence of a proper scaling curve for the B dependence we have fitted a parabola, and estimate that G_0 is 12% higher than G_0^N. Because the field reduces both G^{SC} and G_0^N the 12% represents an upper bound on the error. This is still smaller than the measurement uncertainty as indicated by the bars; we therefore believe the influence of the unwanted Zeeman splitting does not falsify our claim of Kondo universal scaling.

The authors would like to thank Mikio Eto, Christopher Yorke, Yshai Avishai, Wolfgang Belzig, and Leo Kouwenhoven for helpful discussions and/or comments, and Katsuharu Yoshida for technical support. We acknowledge financial support from SORST-JST, NanoQUINE and the Grant-in-Aid for Scientific Research A (No. 40302799 and No. 18201027).

*tarucha@ap.t.u-tokyo.ac.jp

[1] H. E. Stanley, Rev. Mod. Phys. **71**, S358 (1999).
[2] D. C. Ralph, A. W. W. Ludwig, Jan von Delft, and R. A. Buhrman, Phys. Rev. Lett. **72**, 1064 (1994).
[3] A. C. Hewson, *The Kondo Problem to Heavy Fermions* (Cambridge University Press, Cambridge, 1993).
[4] D. Goldhaber-Gordon *et al.*, Nature (London) **391**, 156 (1998).
[5] S. M. Cronenwett *et al.*, Science **281**, 540 (1998).
[6] M. Grobis *et al.*, *Handbook of Magnetism and Advanced Magnetic Materials* (Wiley, New York, 2007), Vol. 5.
[7] D. Goldhaber-Gordon *et al.*, Phys. Rev. Lett. **81**, 5225 (1998).
[8] J. Nygård, D. H. Cobden, and P. E. Lindelof, Nature (London) **408**, 342 (2000).
[9] M. R. Buitelaar, T. Nussbaumer, and C. Schönenberger, Phys. Rev. Lett. **89**, 256801 (2002).
[10] W. Liang, M. P. Shores, M. Bockrath, J. R. Long, and H. Park, Nature (London) **417**, 725 (2002).
[11] A. F. Andreev, Sov. Phys. JETP **19**, 1228 (1964).
[12] Y. Avishai, A. Golub, and A. D. Zaikin, Phys. Rev. B **67**, 041301(R) (2003).
[13] M.-S. Choi, M. Lee, K. Kang, and W. Belzig, Phys. Rev. B, **70**, 020502(R) (2004).
[14] M. Jung *et al.*, Appl. Phys. Lett. **86**, 033106 (2005).
[15] K. Shibata, C. Buizert, A. Oiwa, K. Hirakawa, and S. Tarucha (unpublished).
[16] M. Tinkham, *Introduction to Superconductivity* (McGraw-Hill, Singapore, 1996).
[17] M. R. Buitelaar *et al.* Phys. Rev. Lett. **91**, 057005 (2003).
[18] P. Jarillo-Herrero, J. A. van Dam, and L. P. Kouwenhoven, Nature (London) **439**, 953 (2006).
[19] D. C. Ralph, C. T. Black, and M. Tinkham, Phys. Rev. Lett., **74**, 3241 (1995).
[20] E. Vecino *et al.*, Solid State Commun. **131**, 625 (2004).
[21] T. Sand-Jespersen *et al.*, Phys. Rev. Lett. **99**, 126603 (2007).
[22] K. Grove-Rasmussen, H. I. Jørgensen, and P. E. Lindelof, New J. Phys. **9**, 124 (2007).
[23] M. Pustilnik and L. Glazman, J. Phys. Condens. Matter **16**, R513 (2004).
[24] A. Rosch, J. Kroha, and P. Wölfle, Phys. Rev. Lett. **87**, 156802 (2001).
[25] A. Kaminski, Y. V. Nazarov, and L. I. Glazman, Phys. Rev. B **62**, 8154 (2000).
[26] W. G. van der Wiel *et al.*, Science **289**, 2105 (2000).